Evaluating the Efficiency of Concentric Rings Trajectory for Hyperpolarized ^{13}C MR Spectroscopic Imaging

Wenwen Jiang[1,2], Michael Lustig[3], Martin Uecker[3], and Peder E.Z. Larson[4]

[1]*Graduate Group in Bioengineering, University of California, Berkeley, Berkeley, California, United States,* [2]*University of California, San Francisco, San Francisco, California, United States,* [3]*Electrical Enigneering and Computer Science, University of California, Berkeley, California, United States,* [4]*Radiology and Biomedical Imaging, University of California, San Francisco, California, United States*

Target audience: MR pulse sequence designers, Hyperpolarized ^{13}C MRI, spectroscopic imaging scientists and engineers

Purpose: The powerful feature of hyperpolarized ^{13}C MRSI [1] is that it reflects the altered metabolism in cancer. However, the short-lived effect of hyperpolarization requires rapid and robust imaging techniques. Echo-planar-based spectroscopic imaging (EPSI) techniques and spiral spectroscopic imaging are currently used for acceleration in MRSI. On one hand, the rectilinear sampling pattern of EPSI is less efficient than spirals. In addition, system imperfections induce undesirable spectrum ghosting artifacts for EPSI. On the other hand, the spiral trajectory is very susceptible to eddy currents or gradient delays. Concentric rings k-space trajectory [2,3] provides a powerful alternative for accelerating MRSI. [4] It has advantages of 1) acquisition time saving and 2) robustness to system delay and eddy currents; 3) it is insusceptible to pulsatile flow artifacts, 4) retains the ability of variable density sampling; 5) non-rectilinear circular scanning results in better parallel imaging reconstruction g-factor than Cartesian counterparts. In this work we focus on quantifying and comparing properties of the different sampling patterns and provide both simulations and *in vivo* scans.

Methods: A concentric rings trajectory was designed for 3.8x3.8 mm^2 spatial resolution, 8x8 cm^2 FOV and 500 Hz spectral bandwidth, 10 Hz spectral resolution, as Fig.1 shows. The following acquisition parameters were used: TE/TR=3.4 ms/200 ms, 11 phase-encoded excitations with a progressive flip angle, resulting in a total scan time of 2.2 s, while EPSI required 22 phase encoding excitations and a total scan time of 4.4 s for the same prescriptions. The readout gradients were implemented in gradient echo sequence on a GE Signa 3T scanner. We used min-max NUFFT [5] for reconstruction. We performed normal rat experiments at 35 seconds after an injection of 2.2 mL of 100 mM hyperpolarized [1-^{13}C] pyruvate (using an Oxford Instruments HyperSense polarizer) for both concentric rings and EPSI sequences. Finally, to demonstrate better performance of future parallel imaging application, a Monte-Carlo technique was used to calculate g-factor maps of a simulated 8-channel phased-array coil and 4-fold undersampling.

Results: In the *in vivo* hyperpolarized ^{13}C MRSI study, we compared concentric rings to symmetric EPSI on the same slice with the same prescriptions (Fig.2). Owing to the two-direction sampling pattern of EPSI, eddy currents or any gradient delay results in some ghosting in the spectrum, as Fig.3 shows. In addition to ghosting, EPSI also suffers from pulsatile flow artifacts that are more benign for concentric rings. As confirmed by the g-factor map (Fig.4), the concentric rings trajectory utilizes the sensitivity maps in all directions, which lowers the g-factor noise amplification and also makes it more uniformly distributed.

Conclusion: Our phantom studies and *in vivo* scans demonstrate the potential of using concentric rings in hyperpolarized ^{13}C MRSI for a two-fold acceleration over EPSI, and robustness to flow artifacts and gradient system delay and eddy currents. This isotropic trajectory is also a good fit for parallel imaging.

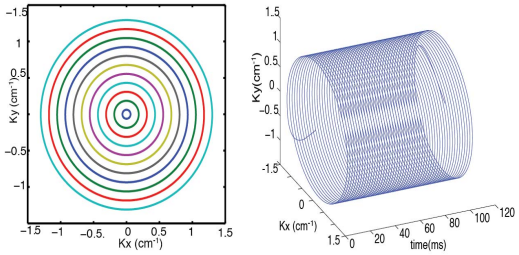

Fig.1. (left) Spatial k-space coverage of all rings; (right) A single ring retraced over time

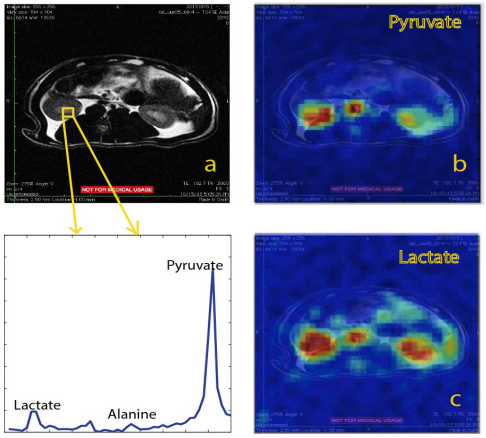

Fig.2. In vivo results using concentric rings from normal rats (axial): a. proton image; b. ^{13}C pyruvate image; c. ^{13}C lactate image

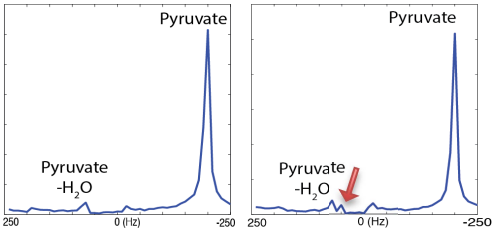

Fig.3. Spectrum from the same voxel from in vivo rat study: (left) concentric ring; (right) EPSI: red arrow shows the spectrum aliasing

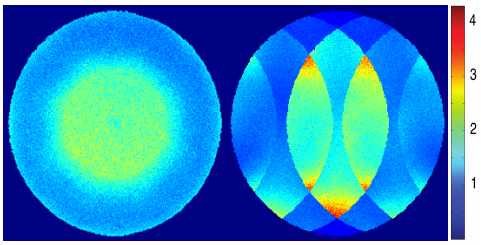

Fig.4. G-factor map with 4x undersampling: (left) concentric rings; (right) Cartesian

References:

[1] Kurhanewicz J, et al. Neoplasia 2011: Nov: VOL.13, NO.2. [2] Wu. H. [D] Stanford University, 2009. [3] Furuyama J, et al. MRM 2012; 67:1515–1522. [4] Jiang, W, Lustig, M and Larson, E.Z. P. ISMRM 2013, #1914. [5] Fessler J, et al. IEEE Trans 2003:Feb: VOL. 51, NO. 2.